# Journal Pre-proof


Vasoactive intestinal polypeptide plays a key role in the microbial-neuroimmune control of intestinal motility

Xiaopeng Bai, Giada De Palma, Elisa Boschetti, Yuichiro Nishihara, Jun Lu, Chiko Shimbori, Anna Costanzini, Zarwa Saqib, Narjis Kraimi, Sacha Sidani, Siegfried Hapfelmeier, Andrew J. Macpherson, Elena F. Verdu, Roberto De Giorgio, Stephen M. Collins, Premysl Bercik

PII: S2352-345X(23)00211-4
DOI: https://doi.org/10.1016/j.jcmgh.2023.11.012
Reference: JCMGH 1271

To appear in: *Cellular and Molecular Gastroenterology and Hepatology*
Accepted Date: 27 November 2023

Please cite this article as: Bai X, De Palma G, Boschetti E, Nishihara Y, Lu J, Shimbori C, Costanzini A, Saqib Z, Kraimi N, Sidani S, Hapfelmeier S, Macpherson AJ, Verdu EF, De Giorgio R, Collins SM, Bercik P, Vasoactive intestinal polypeptide plays a key role in the microbial-neuroimmune control of intestinal motility, *Cellular and Molecular Gastroenterology and Hepatology* (2024), doi: https://doi.org/10.1016/j.jcmgh.2023.11.012.

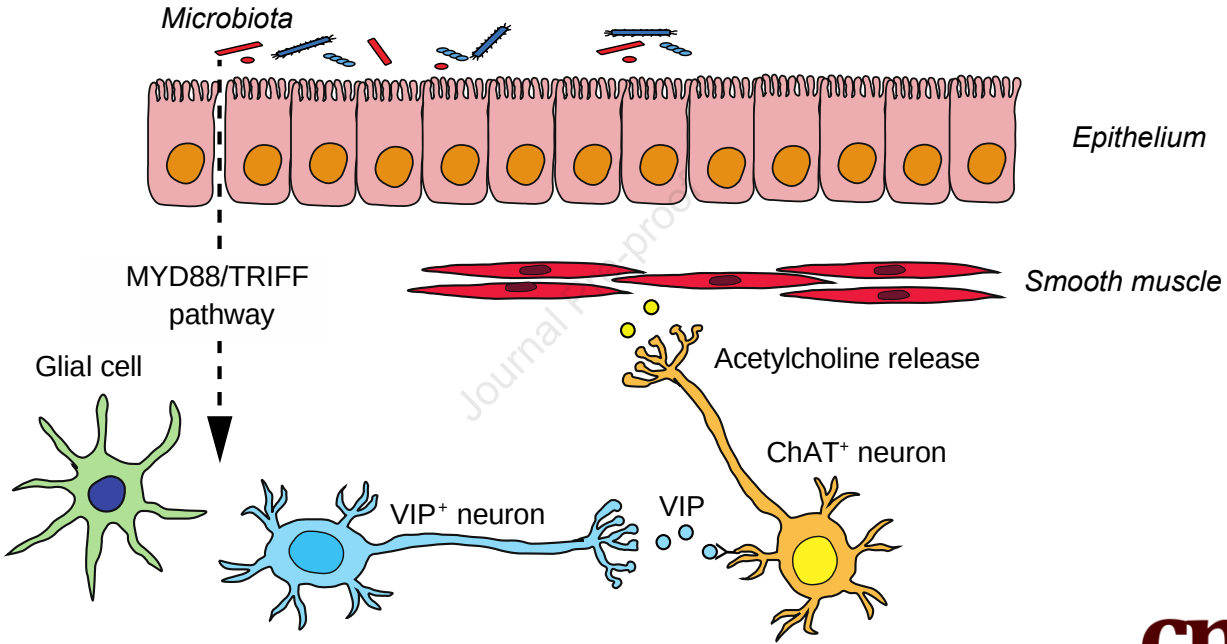




cmgh CELLULAR AND MOLECULAR GASTROENTEROLOGY AND HEPATOLOGY

# Vasoactive intestinal polypeptide plays a key role in the microbial-neuroimmune control of intestinal motility

Short title: Microbiota regulates intestinal motility via VIP

**Xiaopeng Bai**[1, 2], Giada De Palma[1], Elisa Boschetti [3], Yuichiro Nishihara[1], Jun Lu[1], Chiko Shimbori[1], Anna Costanzini[4], Zarwa Saqib[1], Narjis Kraimi[1], Sacha Sidani[1], Siegfried Hapfelmeier[5], Andrew J Macpherson[6], Elena F. Verdu[1], Roberto De Giorgio[7], Stephen M Collins[1], Premysl Bercik[1]

[1]Farncombe Family Digestive Health Research Institute, Department of Medicine, McMaster University, Hamilton, Ontario, Canada.

[2]Department of Medicine and Bioregulatory Science, Graduate School of Medical Sciences, Kyushu University, Fukuoka, Japan

[3]Department of Biomedical and NeuroMotor Sciences, University of Bologna, Bologna, Italy

[4]IRCCS Azienda Ospedaliero-Universitaria di Bologna, Bologna, Italy

[5]Institute for Infectious Diseases, University of Bern, Switzerland

[6]Department of Biomedical Research, University Hospital of Bern, Switzerland

[7]Department of Translational Medicine, University of Ferrara, Ferrara, Italy

**Address correspondence to**:
Premysl Bercik, MD
Farncombe Family Digestive Health Research Institute, Department of Medicine, McMaster University, HSC 3N9, Hamilton, Ontario, Canada.
Tel: 905-525-9140 ext. 73495,
Email: bercikp@mcmaster.ca

**Author contributions:**

Xiaopeng Bai: Conceptualization, Methodology, Writing - Original Draft, Review & Editing
Giada De Palma: Methodology, Software, Investigation, Writing- Review & Editing
Elisa Boschetti: Resources, Data Curation
Jun Lu: Methodology
Yuichiro Nishihara: Investigation
Chiko Shimbori: Methodology
Anna Costanzini: Resources, Data Curation
Zarwa Saqib: Investigation
Narjis Kraimi: Investigation
Sacha Sidani: Investigation
Siegfried Hapfelmeier: Resources
Andrew J Macpherson: Resources, Writing - Review & Editing
Roberto De Giorgio: Supervision, Project administration, Writing - Review & Editing
Elena F. Verdu: Resources, Writing - Review & Editing
Stephen M Collins: Supervision, Project administration, Writing - Review & Editing, Premysl Bercik: Supervision, Project administration, Writing - Review & Editing, Funding acquisition

**Synopsis**

We have identified a novel neuroimmune mechanism, by which gut microbiota regulates intestinal motility that can lead to development of new treatments, including microbial therapeutics, targeting small intestinal VIP to treat chronic constipation and diarrhea.

**Keywords**:

Gastrointestinal motility; microbiota; enteric nervous system; vasoactive intestinal polypeptide.

**Acknowledgments:**

Funding by Canadian Institutes of Health Research grant #143253 (to PB and SMC). PB holds the Richard Hunt-AstraZeneca Chair in Gastroenterology.

**Conflict of interests:**

There are no relevant conflicts of interest to declare.

## Abstract

**Background and Aims:** Although chronic diarrhea and constipation are common, the treatment is symptomatic as their pathophysiology is poorly understood. Accumulating evidence suggests that the microbiota modulates gut function but the underlying mechanisms are unknown. We therefore investigated the pathways by which microbiota modulates gastrointestinal motility in different sections of the alimentary tract.

**Methods:** Gastric emptying, intestinal transit, muscle contractility, acetylcholine release, gene expression and vasoactive intestinal polypeptide (VIP) immunoreactivity were assessed in wild-type and *Myd88*$^{-/-}$*Trif*$^{-/-}$ mice in germ-free, gnotobiotic and SPF conditions. Effects of transient colonization and antimicrobials, as well as immune cell blockade were investigated. VIP levels were assessed in human full thickness biopsies by Western blot.

**Results:** Germ-free mice had similar gastric emptying but slower intestinal transit compared with SPF mice, or mice monocolonized with *Lactobacillus rhamnosus* or *Escherichia coli,* the latter having stronger effects. While muscle contractility was unaffected, its neural control was modulated by microbiota by upregulating jejunal VIP, which co-localized with and controlled cholinergic nerve function. This process was responsive to changes in the microbial composition and load, and mediated through TLR signaling, with enteric glia cells playing a key role. Jejunal VIP was lower in patients with chronic intestinal pseudo-obstruction compared with control subjects.

**Conclusion:** Microbial control of gastrointestinal motility is both region- and bacteria-specific, it reacts to environmental changes, and is mediated by innate immunity-neural system interactions. Small intestinal VIP, by regulating cholinergic nerves, plays a key role in this process, thus providing a new therapeutic target for patients with motility disorders.

## Introduction

Although functional diarrhea and constipation are very common, their treatment is symptomatic, as the pathophysiology is not well understood[1]. This is in part due to our limited understanding of basic mechanisms governing gastrointestinal motility, including complex neuro-immune networks and microbial-host interactions[2].

The role of microbiome in determining gut function has emerged during the last decades. It is now well established that the microbiome shapes the mucosal immune system, regulates intestinal barrier, and affects visceral sensitivity and gastrointestinal motility[3-5]. Early studies demonstrated that germ-free rats have slower gastrointestinal transit compared to conventional rats[6]. Developmental studies then showed that during gestation bowel movements are weak but begin to normalize after birth[7], accompanying microbial colonization and consequent maturation of the enteric nervous system (ENS). Gut microbiota affects the ENS and colonic motility by signaling through toll like receptors (TLRs)[8, 9], which are expressed by neurons and glial cells[10], as well as by maturation of colonic serotonin-containing cells and neural networks[11, 12].

Although the accumulated data suggest that microbial-neuro-immune interactions play a key role in the gastrointestinal motility, the precise mechanisms are incompletely understood. Most previous work focused on the colon, as the site of the highest bacterial biomass, while the small intestine with the highest density of immune cells in the digestive tract[13] has received relatively little attention [14]. Furthermore, microbial-neuro-immune mechanisms controlling motility likely differ between different sections of the digestive tract, reflecting different functions in sequential food processing, digestion, storage, and waste elimination.

Here we show that small intestinal motility, but not gastric emptying or colonic motility, is

regulated by the microbiome through modulation of vasoactive intestinal polypeptide (VIP) that controls cholinergic nerve function. We demonstrate that this process is dynamic, dependent on TLR signaling and likely mediated by enteric glial cells.

**Results**:

***Gut microbiota modulates intestinal transit but not gastric emptying***

There was no difference in gastric emptying between specific pathogen-free (SPF) mice, germ-free mice, mice monocolonized with non-pathogenic *Escherichia coli JM83* or *Lactobacillus rhamnosus X-32.2* (Fig. 1A). However, intestinal transit was slower in germ-free mice, with most metallic beads found in the small intestine, compared to SPF mice or mice monocolonized with *E. coli* or *L. rhamnosus,* in which the beads were mainly localized in the cecum or colon (Fig 1B). Even though both groups of mono-colonized mice showed faster intestinal transit than germ-free mice, it was more pronounced in *E. coli-monocolonized* mice (Fig. 1B), suggesting a differential modulation of gut function by specific bacterial strains.

***Gut microbiota regulates intestinal contractility through cholinergic nerves***

To investigate underlying mechanisms, we studied jejunal and colonic tissue contractility *in vitro*. Equivalent KCl- or carbachol (CCh)-stimulated muscle contractility in all groups indicated that myogenic function was unaffected by the gut microbiota (Fig. 1C,D). To assess neural regulation, we used electric field stimulation (EFS)[15], in the presence or absence of tetrodotoxin or atropine. In SPF mice, EFS induced both jejunal and colonic contractility; this was preceded by strong relaxation in the colon, and minor relaxation in the jejunum (Fig. 1E,F). Tetrodotoxin blocked EFS-induced responses, confirming a neurogenic origin. Atropine administration decreased contractions both in the jejunum and colon, and magnified the initial relaxation in the jejunum (Fig. 1E,F), suggesting it is under cholinergic control.

The initial EFS-induced jejunal relaxation was much stronger in germ-free compared with SPF

mice, or mice colonized with *E. coli*, whereas these microbiotas promoted EFS-stimulated contraction in the colon (Fig. 1G,H), indicating that cholinergic nerves are regulated by the microbiota in a region-specific manner. Unlike *E. coli*-monocolonized animals, responses in *L. rhamnosus*-monocolonized mice were not different from those of germ-free mice (Fig. 1G,H), indicating that specific bacterial species exert different effects on the host. EFS-induced [3H]-acetylcholine release[16] in the jejunum was lower in germ-free mice compared to SPF and *E. coli*-monocolonized mice, but similar to *L. rhamnosus*-monocolonized mice (Fig. 1I). We observed a similar pattern in the colon but differences with selectively colonized mice did not reach statistical significance. Altogether, these data suggest that the presence of specific gut microbiota distinctly affect functional responses driven by the cholinergic system in the small intestine and the colon.

***Gut microbiota regulates VIP control of cholinergic nerves***

To identify putative mediators, we analyzed whole tissue gene expression in the jejunum and colon using a custom-designed Nanostring Codeset, that included genes related to regulation of muscle contractility, such as choline acetyltransferase (*ChAT*), substance P (*Sp)*, *Vip* and nitric oxide synthase (*Nos*) (Fig. 2 A,B). Whilst there were no significant differences in *ChAT*, *Sp* or *Nos* gene expression, *Vip* expression was lower in GF compared to SPF mice (Fig. 3A,B). To verify the role of VIP in contractility, we pre-treated intestinal tissues from SPF mice by combining VIP receptor 1 and 2 antagonists and then stimulated them with EFS. Pretreated jejunal tissues displayed increased relaxation and decreased contraction, while no significant effect was observed in the colon (Fig. 3C), confirming that VIP regulates the activity of small intestinal

157 cholinergic neurons as suggested by a previous study[17]. To explore *in vivo* effects of VIP, we
158 administered a VIP analogue or saline to SPF mice using osmotic pumps. Mice that received the
159 VIP analogue had faster intestinal transit (Fig. 3D), further supporting the stimulatory role of VIP
160 in intestinal motility.

161 To validate the expression of VIP and ChAT in the myenteric plexus, we performed
162 immunofluorescence staining with anti-VIP, anti-ChAT and anti-Hu antibodies. VIP-
163 immunoreactive neurons and ChAT-immunoreactive neurons co-localized in the myenteric plexus
164 of the jejunum of SPF mice (Fig. 3E). While the ChAT immunoreactivity levels were similar
165 between SPF and germ-free mice (Fig. 3F), in agreement with our gene expression data, VIP
166 levels differed between GF, SPF, and *E. coli*-monocolonized mice (Fig. 3G), mirroring the
167 intestinal transit results.

168 Although VIP gene expression in full thickness colonic tissues was higher in SPF mice compared
169 to germ-free mice (Fig. 2B), VIP immunoreactivity in colonic myenteric plexus was similar
170 between germ-free and SPF mice (Fig. 3H), likely reflecting changes in the mucosal or
171 submucosal layers, ostensibly not related to the motility control.

172

173 ***The innate immune system modulates intestinal VIP expression***

174 As neuroimmune interactions play a key role in gut function[18, 19], and MYD88-TRIF signaling
175 is critical for TLR-mediated immune responses to bacteria[20, 21], we analyzed these gene
176 expression in GF and SPF mice. Jejunal *Tollip* and *Myd88* expression differed between GF and
177 SPF mice (Fig. 2A), therefore we assessed motility in *Myd88*$^{-/-}$*Trif*$^{/-}$ and wild type (WT) mice.
178 Although intestinal transit and jejunal EFS-induced contractility were similar between knockout

and wild type mice in the absence of microbiota, they differed between WT and *Myd88*$^{-/-}$ *Trif*$^{-/-}$ colonized mice (Fig. 4A,B). VIP expression in jejunal myenteric plexus mirrored these results, with similar levels in germ-free conditions and higher levels in SPF WT mice (Fig. 4C).

To validate these results, we assessed motility and contractility in GF *Myd88*$^{-/-}$*Trif*$^{-/-}$ and WT mice, before and after monocolonization with *E. coli*. While there were no differences between the two strains in germ-free condition, *E. coli*-monocolonization increased intestinal transit and EFS-induced jejunal contractility in WT mice (Fig. 4E,F), with no changes in *Myd88*$^{-/-}$*Trif*$^{-/-}$ mice. In parallel, *E. coli*-monocolonization increased VIP immunoreactivity in WT, but not in *Myd88*$^{-/-}$ *Trif*$^{-/-}$ mice (Fig. 4G,H), suggesting that the microbiota regulates small intestinal motility by modulating myenteric VIP expression through TLR-dependent pathways.

***Microbial modulation of glial cells underlies changes in VIP expression***

To investigate the role of innate immune cells in this process, we used fingolimod, a sphingosine-1-phosphate receptor modulator that inhibits activation and migration of immune cells, including dendritic and enteric glial cells, and cosalane that blocks activation of dendritic cells through CCR7[22-24]. Fingolimod, but not cosalane, decreased myenteric VIP levels in *E. coli*-monocolonized mice (Fig. 5B).

We then investigated presence of glial cells, identified by S100 calcium binding protein B (S100β) and glial fibrillary acidic protein (GFAP) immunoreactivity, and found they were co-localized with VIP nerves in SPF mice (Fig. 5A). Similar to VIP expression, fingolimod, but not cosalane, attenuated the expression of myenteric S100β in *E. coli*-monocolonized mice (Fig. 5C). Furthermore, mirroring the results of intestinal transit and VIP expression, SPF and *E. coli*-

monocolonized mice had higher S100β levels than germ-free mice (Fig. 5D).

To further explore the role of enteric glial cells in motility control, we used gliotoxin to inhibit their function. One-week intraperitoneal administration of gliotoxin in SPF mice resulted in a prolonged intestinal transit time accompanied by a decrease in VIP expression in the jejunal myenteric plexus (Fig. 5E,F). All together, these data suggest that microbiota-glial cells interactions underlie changes in VIP expression and intestinal motility.

***Presence of microbiota is essential for normal intestinal motility***

To study whether the continuous presence of microbiota is required for regular intestinal VIP levels and gut motility, we used the transient bacterial colonizer *E. coli HA107*[25] or treatment with non-absorbable antibiotics. Ex-germ-free mice gavaged with *E. coli HA107* (Fig. 6B) displayed faster intestinal transit and higher VIP levels at day 14 post-colonization, when bacteria were present in the gut. However, at day 42, after reverting to the germ-free status, the intestinal transit and VIP expression decreased (Fig. 6B). In contrast, mice mono-colonized with *E. coli JM83* (wild type) displayed faster intestinal transit and higher VIP levels both at day 14 and 42 post-colonization compared to germ-free mice (Fig. 6A).

Administration of broad spectrum antibiotics to SPF mice (Fig. 6C), resulted in slower intestinal transit and lower jejunal myenteric VIP-immunoreactivity, both of which normalized two weeks later (Fig. 6C). Antibiotics, as shown previously[26], altered microbial profiles and reduced total bacterial counts (Fig. 6D,E), which normalized 2 weeks later. This suggests that continuous presence of bacteria is required for normal motility, and that changes in the microbial load and profiles are dynamically reflected by changes in intestinal transit and myenteric VIP.

223

224 ***Small intestinal VIP is decreased in patients with severe constipation***

225 To illustrate the clinical relevance of our findings, we examined VIP expression in full thickness
226 biopsy samples of small intestinal tissues from patients with established chronic intestinal pseudo-
227 obstruction (CIPO), which is characterized by intractable constipation. Compared with small
228 intestinal samples from control subjects, VIP expression was lower in CIPO specimens (Fig. 6F),
229 providing further support for its role in the regulation of gastrointestinal motility.

230

## Discussion

While the key role of microbiota in regulating gastrointestinal motility is well established, the precise mechanisms are poorly understood. We show that gastric emptying is not affected by the microbiota, while intestinal transit differs between germ-free and colonized mice. The changes in transit are determined by the altered function of the small intestine, as most metallic beads were found in the jejunum and ileum. This was not due to the changes in myogenic function, as KCl-stimulated muscle contractility was similar between germ-free and colonized mice, but due to changes in its neural control. EFS-induced contraction and relaxation patterns were affected by the microbiota, with more pronounced relaxation and weaker contraction in germ-free mice, paralleled by acetylcholine release. Microbial influence differs between bacterial strains, as intestinal transit, acetylcholine release and contractility were lower in *L. rhamnosus*-monocolonized mice compared to those with *E. coli* or complex SPF microbiota.

When investigating underlying mechanisms, there was no difference in ChAT expression between germ-free and SPF mice, suggesting that cholinergic nerves are not affected *per se*, but we found major differences in VIP gene expression. VIP acts on receptors located on smooth muscle to mediate relaxation[27] but it also serves as a co-transmitter at cholinergic synapses in the small intestinal myenteric plexus[17], activating jejunal cholinergic neurons[28]. Accordingly, VIP-deficient mice display decreased jejunal motility[29], while VIP administration enhances motility as demonstrated previously[30] and in our study, supporting its role in excitatory pathways. We observed co-localization of jejunal myenteric VIP- and ChAT-immunoreactive neurons and found that pretreatment with VIP receptor antagonists increased relaxation and decreased contraction of jejunal tissues, demonstrating that VIP controls cholinergic nerves in the small intestine.

VIP is mainly expressed in the myenteric plexus, but it is also abundant in mucosal and submucosal layers[28, 31]. Colonic myenteric VIP immunoreactivity was not altered by the gut microbiota, but VIP gene expression was affected in whole thickness colon tissues. This is in agreement with studies demonstrating that microbiota does not alter colonic myenteric VIP expression[12], that colonic VIP receptors mainly localize at the mucosa[32] and that VIP gene mutation is associated with minimal changes in the colon function[29]. Thus, while the effect of the microbiota on VIP expression in the colon is exerted in the mucosal layer, promoting colonic barrier homeostasis[33], in the small intestine the VIP is linked to motility and cholinergic nerve control.

To further investigate the mechanisms underlying changes in intestinal motility, we colonized germ-free mice with a single Gram-negative (*E. coli*) or Gram-positive (*Lactobacillus rhamnosus*) bacterial strain. Though more significant in *E. coli*-colonized group, both increased small intestinal motility and VIP expression, confirming that both TLR4 and TLR2 pathways are involved in microbial control of gut motility and neural function[8, 9]. MYD88/TRIF signaling pathways are downstream from both TLR 2 and 4 receptors, playing key roles in host innate immune responses to bacteria[21, 34, 35]. We found that *Myd88* gene expression differed between GF and SPF mice in wild type mice, and that intestinal transit, jejunal contractility and myenteric plexus VIP immunoreactivity were similar in germ-free and SPF *Myd88*$^{-/-}$*Trif*$^{-/-}$ mice. Furthermore, *E. coli*- monocolonization of germ-free *Myd88*$^{-/-}$*Trif*$^{-/-}$ mice did not alter these parameters, demonstrating that TLR-signaling mediates the microbial control of intestinal motility.

To identify innate immune cells involved in this process we used cosalane, which specifically inhibits dendritic cell activation[24, 36], and fingolimod that inhibits activation and migration of immune cells, including dendritic and enteric glial cells[37-39]. We found that fingolimod, but

not cosalane, blocked increase in VIP expression after bacterial colonization, suggesting that enteric glial cells, rather than dendritic cells, are involved in this process. Enteric glial cells contribute to gut function maintenance, including motility, synaptic transmission and neurogenesis, via dynamic interactions with immune cells and neurons[40, 41]. Indeed, we found that glial cells shared the same localization and changes in density as VIP positive neurons, suggesting that they mediate the bacterial control of intestinal motility. Furthermore, specific inhibition of glial cell function with gliotoxin decreased VIP expression and prolonged intestinal transit time, further supporting the key role of glial cells. A denser immune cell network in the small intestine [42] and possibly different functional phenotypes of enteric glial cells in the small intestine compared to the colon [43], might be the reason why the microbial-immune crosstalk governs gastrointestinal motility mainly in the small intestine and not in the colon.

Immune responses can be long-lived in transiently colonized mice[25], but it is unknown whether they are sufficient to maintain normal motility. We used *E. coli HA107,* a triple auxotrophic mutant that colonizes the mouse intestine only transiently and is not detectable 48 hours after its last gavage[25], to monocolonize germ-free mice. While intestinal transit and VIP expression increased during colonization, both returned to values observed in germ-free mice four weeks later, suggesting that the immune priming associated with the microbial colonization is not sufficient, and that bacterial presence is needed to maintain normal intestinal motility.

The microbiota is involved in the maturation of enteric nervous system[11] and maintenance of its homeostasis[44]. In our experiments, administration of non-absorbable antimicrobials to SPF mice decreased jejunal VIP levels and intestinal transit, which then normalized two weeks later, in parallel with microbiota profiles. This demonstrates that VIP expression in adult, conventionally raised mice, is continuously and dynamically modulated by the gut microbiota.

To validate our findings clinically, we investigated levels of small intestinal VIP in a small set of patients with chronic intestinal pseudo-obstruction (CIPO). CIPO is the 'tip of the iceberg' of a wide spectrum of gastrointestinal motility disorders, and CIPO-affected patients suffer from intractable constipation[45]. We found that compared with control subjects, jejunal VIP levels are lower in patients with CIPO, thus extending our findings from mouse models into humans. These results are in agreement with multiple reports demonstrating that intestinal VIP is lower in patients with chronic constipation and higher in those with chronic diarrhea[46, 47]. Interestingly, recent studies suggested that fecal microbiota transplantation improves symptoms in patients with intestinal dysmotility, including those with Irritable Bowel Syndrome and CIPO[48, 49], and we hypothesize that these beneficial effects, might be, at least in part, due to the microbial regulation of intestinal VIP.

In summary, we show that gut microbiota regulates gastrointestinal motility in a region-specific manner, with maximum effects seen in the small intestine. Specific bacterial strains exert differential effects, with major changes seen with *E. coli* and minimum ones with *L. rhamnosus*. Gut microbiota affects the function and structure of the jejunal ENS by modulating myenteric VIP, which in turn controls cholinergic nerves. This regulation is dependent on microbiota-innate immune system crosstalk, critically involving MYD88/TRIF-dependent pathways and enteric glia cells. Both the presence and stability of microbiota are essential to maintain myenteric VIP level and normal intestinal motility. Finally, we show that jejunal VIP levels are altered in patients with severe constipation, thus providing clinical relevance to our murine experiments.

Our data suggest that deeper understanding of microbiota-neuroimmune interactions in the small bowel could lead to better therapies to manage motility disorders. These could include identification and development of microbial therapeutics that modulate small intestinal VIP to

322 treat chronic constipation and diarrhea.

323

## Methods

All animal experiments were approved by the McMaster University Animal Care Committee (AUP 18-08-35). The clinical study was approved by the Ethics Committee of St. Orsola-Malpighi Hospital of Bologna, Italy (Protocol No. 50/2012/O/Sper (EM/146/2014/O)). All patients and healthy controls provided written informed consent to participate.

### *Gnotobiotic mice*

*MyD88*$^{-/-}$*; Ticam1*$^{-/-}$ mice on a C57BL/6 background were kindly provided by B. A. Beutler (La Jolla, CA, USA). SPF C57BL/6 mice were purchased from Taconic. Germ-free C57BL/6 and *MyD88*$^{-/-}$*; Ticam1*$^{-/-}$ mice were rederived at the Farncombe Family University Axenic Gnotobiotic Unit (AGU) of the Central Animal Facility, McMaster University, and maintained axenic in sterile isolators. To ensure sterility, handling of GF mice was carried out under axenic conditions, as described previously[50]. All mice were maintained on a 12-hour day/night cycle with free access to food and water. GF and mono-colonization status was assessed regularly by direct bacteriology, immunofluorescence and 16S PCR testing for culturable and unculturable organisms.

### *Bacterial colonization of germ-free mice*

Germ-free mice (both sexes) were monocolonized with $10^9$ CFU of *E. coli JM83*, *Lactobacillus rhamnosus X-32.2* or *E. coli HA107* via intragastric gavage (200 µl/mouse). *E. coli HA107* strain is a mutant form of the parental strain *E. coli JM83*, which is not able to synthesize meso-

diaminopimelic acid (m-DAP, Sigma-Aldrich) or D-isomer of alanine (D-Ala, Sigma-Aldrich) required in the peptidoglycan crosslink of the cell wall and thus only transiently colonizes (12-48 hours) mouse intestine[25]. The transient colonizer *E. coli HA107* was gavaged three times weekly for two weeks (Fig. 6B). The permanent colonizer *E. coli JM83* (Fig. 6A) and *Lactobacillus rhamnosus X-32.2* were gavaged once. All mono-colonized mice were maintained in sterile isolators within the Axenic Gnotobiotic Unit.

*E. coli JM83* was grown in Luria Bertani (LB) broth (Sigma-Aldrich) and *E. coli HA107* was grown in LB broth supplemented with D-Ala (200µg/ml)/m-DAP (50µg/ml), and incubated with shaking at 160 rpm at 37°C for 12 hours. *Lactobacillus rhamnosus X-32.2* was grown in deMan, Rogosa and Sharpe (MRS) broth, anaerobically, at 37°C for 18 hours. Bacteria were harvested by centrifugation (15 min, 3500X g) in a 400 ml sterile flask, washed in sterile PBS and concentrated, all under a sterile laminar flow hood. The bacterial suspensions were sealed in sterile tubes, with the outside surface kept sterile, and imported into sterile isolators.

To assess colonization or *de novo* GF status after transient colonization, cecal contents were plated on LB agar plates (with or without supplementation with m-DAP and D-Ala), or on MRS agar plates and incubated for 48 hours.

To confirm the colonization efficiency of *E. coli JM83* and *L. rhamnosus*, the ceca from 5 mice per group were thawed and the contents diluted 10 times (w/v) with sterile PBS, then serially diluted again (10-fold) with PBS until $10^{-9}$. Diluted samples (100 ul; diluted to $10^{-9}$, $10^{-7}$ and $10^{-5}$) were then plated onto MRS (for *L. rhamnosus*) or BHI (for *E. coli JM83*) plates and incubated aerobically or anaerobically during 48 hours. After 48 hours the colonies that grew on the plates were counted and CFU/mL calculated. We saw no differences in the colonization levels between

the two bacterial strains ($4.82 \times 10^9 \pm 3.71 \times 10^9$ for *E. coli JM83*; $3.44 \times 10^{10} \pm 4.58 \times 10^{10}$ for *L. rhamnosus*).

***Gnotobiotic husbandry***

Isolators that housed GF mice underwent strict protocols to prevent contamination of microbes from animal handlers or environment. Samples of the imported materials were taken for aerobic and anaerobic bacterial culture regularly. Feces and bedding were taken from the isolator for direct bacteriology, microscopy and 16S PCR testing of intestinal contents to test for culturable and unculturable organisms. Cecal contents from mono-colonized mice were suspended and serially diluted in sterile 1X PBS and plated on LB or MRS agar plates for 48 hours. Cecal contents from mice treated with *E. coli HA107* strain were incubated on LB plates supplemented with m-DAP and D-Ala. To confirm *de novo* GF status after colonizing with *E. coli HA107*, cecal contents were plated on supplemented LB agar plate 2 and 4 weeks after the last gavage.

***Antibiotics administration***

Neomycin (Sigma-Aldrich) and bacitracin (Sigma-Aldrich) were dissolved in distilled water (both at 5 mg/mL), pimaricin (Sigma-Aldrich) added (5 µL/mL) and the solution filtered sterile. Antibiotics were administered for 1 week and changed every 48 hours.

***Gastric emptying***

Gastroduodenal motility was assessed using video image analysis as described previously[51].

Briefly, mice were gavaged with 0.2 ml of 40% barium solution, placed in custom Plexiglas restrainers and videofluoroscoped for 4 min. Video images were analyzed using ImageJ. Gastric emptying was assessed in single images by manually outlining the border of stomach and measuring gastric area and its mean optical density. The amount of barium at 0 and 4 minutes was assessed by multiplying the gastric area by the mean optical density in each image Gastric emptying was expressed as a percentage of barium expelled from the stomach in 4 min.

***Gastrointestinal transit***

Gastrointestinal transit was assessed using videofluoroscopy as described previously[52]. Briefly, five steel beads (0.79 mm diameter; Bal-tec.) with 40% barium solution (0.1 ml) were gavaged into each mouse. A second barium gavage (0.2 ml) was performed 170 min later. Ten minutes later, the mouse was placed in a custom-built Plexiglas restrainer and videofluoroscoped. Video images were analyzed using ImageJ. Each bead was assigned a score depending on its location within the gastrointestinal tract and their scores added together to calculate a total transit score.

***Gene expression***

RNA was extracted by RNeasy Mini Kit (Qiagen, Toronto, Canada), DNase digestion was performed by RNase-free DNase (Qiagen). A custom Nanostring codeset ran according to manufacturer's instructions was analyzed by nSolver 4.0 (NanoString Technologies, Seattle, WA) and by Ingenuity Pathway software (Qiagen).

409 ***Muscle contractility***

410 Muscle contractility was assessed as previously described[53], after stimulation with KCl,
411 carbachol, electric field stimulation and VIP receptor antagonist 1 (Acetyl-(D-
412 Phe$^{2}$,Lys$^{15}$,Arg$^{16}$,Leu$^{27}$)-VIP(1-7)-GRF(8-27)trifluoroacetate, 10 μM) and 2 (VPAC2):Myristoyl-
413 (Lys$^{12,27,28}$)-VIP-Gly-Gly-Thr-trifluoroacetate, 10 μM; Bachem, CA, USA), using multichannel
414 transducer system (MLT0201, Panlab s.l, Spain).

415 Muscle contractility was measured as previously described[53]. Briefly, tissue of the jejunum and
416 mid colon were kept in oxygenated (95% $O_2$, 5% $CO_2$) Krebs solution containing (in mM) 120.9
417 NaCl, 1.2 $NaH_2PO_4$, 15.5 $NaHCO_3$, 5.9 KCl, 2.5 $CaCl_2$, 1.2 $MgCl_2$, and 11.1 glucose, at pH 7.4.
418 One centimeter sections of the gut were removed from the jejunum, beginning at the ligament of
419 Treitz and proceeding distally, and mid colon. The lumen of each segment was flushed gently with
420 Krebs buffer before the insertion of short Silastic tubing (0.065 in. OD, 0.030 in. ID; Dow Corning,
421 Midland, MI) into each end. The tubing was then tied in position with surgical silk. Segments
422 were hung in the longitudinal axis and attached to a force transducer (MLT0201, 5mg-25g, Panlab
423 s.l, Spain). Tissues were equilibrated for 30 min in oxygenated Kreb's solution and then stretched
424 with 1 mg force before the experiment was started. Muscle strips were then stimulated with 50
425 mM KCl, carbachol, VIP receptor antagonists and electric field stimulation (EFS, 30 V, 5 Hz,
426 0.5 mS) and responses were recorded. VIP receptor antagonists of type 1 (VPAC1), Acetyl-(D-
427 Phe$^{2}$, Lys$^{15}$, Arg$^{16}$, Leu$^{27}$)-VIP(1-7)-GRF(8-27) trifluoroacetate salt and antagonists of type 2
428 (VPAC2): Myristoyl-(Lys$^{12,27,28}$)-VIP-Gly-Gly-Thr(free acid) trifluoroacetate salt were
429 purchased from Bachem Inc (CA, USA). The force was expressed in percent, assigning the levels
430 obtained at rest and at peak of KCl-induced contraction as 0% and 100%, respectively.

### *[$^3$H]-choline release measurement*

Small intestine and colon were removed and cut in half. Longitudinal muscle–myenteric plexus preparations were dissected, placed in oxygenated Krebs' solution and pre-incubated with 0.5 µmol/l of [$^3$H]-choline for 40 min at 37 °C as previously described[16, 52]. Tissues were then transferred to the superfusion chambers and perfused with Krebs' solution with 5 mM hemicholinium-3 at a rate of 1 ml$^{-1}$ min. Aliquots were collected every 2 min for 80 min using Spectrum™ Spectra/Chrom™ CF-1 Fraction Collector (FL, USA). [3H]-Acetylcholine release was induced by EFS (30 V, 10 Hz, 0.5 mS) for 1 min (S48 stimulator; Grass, Quincy, MA) or by adding 50 mmol/l KCl to the superfusate for 6 min, and then measured using a Beckman scintillation counter (LS5801; Beckman Instruments, Fullerton, CA) at a counting efficiency of 35% and expressed as a fraction of the total [3H] in the tissue. Acetylcholine release was expressed in %, assigning the levels of choline release at baseline and at peak level induced by KCl as 0% and 100%, respectively.

### *VIP analogue in vivo application*

VIP analogue[54], [Ala2,8,9,11,19,22,24,25,27,28]-VIP (BioCrick BioTech, Chengdu, China), 5µg/day or vehicle (PBS) was administered by continuous subcutaneous infusion at 1 µl/h, for 3 days via osmotic pumps (Alzet Model 2001; Durect Corporation, Palo Alto, CA, USA). The osmotic pump was incubated in PBS for 24 h at 37°C prior to implantation and was implanted dorsally using isoflurane anesthesia. Transit time was measured on day 3.

453 ***Gliotoxin in vivo application***

454 Gliotoxin fluorocitrate solution was prepared as described before[55]. D,L-fluorocitric acid, Ba,
455 salt (Sigma-Aldrich) 8 mg of was dissolved in 1 ml of 0.1 mmol/L HCL. Two to three drops of
456 0.1 mmol/L $Na_2SO_4$ were added to precipitate the $Ba^{2+}$. Two milliliters of 0.1 mmol/L $Na_2HPO_4$
457 was added, and the suspension was centrifuged at 1,000 g for 5 mins. The supernatant was diluted
458 with PBS to the final concentration, and the pH was adjusted to 7.4. The Gliotoxin fluorocitrate
459 solution (20μmol/Kg/day) or PBS was injected intraperitoneally daily for 7 days. Gastrointestinal
460 transit time was measured on days 0 (prior to first injection) and 7.

461

462 ***Immunohistochemistry assessment***

463 Whole mounts of intestine were collected immediately following sacrifice, cut open
464 longitudinally and pinned serosal side down on Petri dishes. The tissues were fixed for 2 hours at
465 room temperature in 4% phosphate-buffered formaldehyde (pH 7.4), then washed in phosphate
466 buffered saline (PBS). Laminar preparations of longitudinal muscle with adherent myenteric
467 plexus were obtained by dissections. Tissues were then permeabilized and blocked by incubation
468 in PBS containing 0.4% Triton X-100 and 5% normal bovine serum. Primary antibodies including
469 rabbit polyclonal IgG antibodies to Vasoactive Intestinal Peptide (VIP: dilution 1:5000;
470 Immunostar), biotinylated mouse monoclonal antibodies to human neuronal protein HuC/HuD
471 (HuC/D: dilution 1:100; Molecular Probes, Invitrogen), goat polyclonal Choline
472 Acetyltransferase antibodies (ChAT, dilution 1:100; Invitrogen), S100 beta antibody (S100$\beta$,
473 dilution 1:500, GeneTex) were applied overnight at 4°C. Antibody binding was detected with
474 donkey anti-rabbit antibodies labeled with Alexa 555 (1:1000; Molecular Probes), streptavidin

labeled with Alexa 488 (1:200; Molecular Probes), donkey anti-goat antibodies labeled with Alexa 555 (1:200; Molecular Probes) or with donkey anti-goat antibodies labeled with Alexa 647 (1:100; Molecular Probes) by incubation for 2 hours at room temperature. No immunostaining was observed when primary antibodies were omitted. Tissue sections were mounted with Vectashield medium (Vector Laboratories Canada Inc., Burlington, ON, Canada). Raw pictures in gray scale were loaded into FIJI ImageJ, signals were normalized by setting threshold as 0-1. Staining level was expressed in percentage, by the ratio of VIP-positive area in a 1 $cm^2$ image.

***Microbiota analysis***

Total genomic DNA was extracted from cecal samples, and the V3 region of the 16S rRNA gene amplified and Illumina sequencing performed as previously described[56, 57]. The data was analyzed following the pipelines of dada2[58], QIIME2[59], and Phyloseq package (1.30) for R (3.6.3)[60]. Taxonomic assignments were performed using the RDP classifier with the Greengenes (2013) training set[61, 62]. Analyses were done using QIIME2, Phyloseq package (1.30), and SPSS software v.23. All results were corrected for multiple comparisons, allowing 5% of False Discovery Rate.

Total bacterial load was measured by qPCR with the primers 926F 5'-AAACTCAAAKGAATTGACGG-3' and 1062R 5'-CTCACRRCACGAGCTGAC-3' for the V6 region of the 16S rRNA. The data was expressed as total bacterial load relative to the average of the control population (baseline water): E (Ct test- Ct calibrator), where E was the efficiency of each PCR (1.97-2), and the calibrator was the average of the Ct of all baseline controls.

497 ***Patient samples***

498 Full-thickness jejunal samples were collected from well-characterized CIPO patients with
499 degenerative neuropathy (total n= 6, female=3, age range: 30-73 years) investigated at St. Orsola-
500 Malpighi Hospital, Bologna, Italy. Control samples were obtained from patients undergoing
501 resection due to non-complicated intestinal tumors (total n= 8, female=3; age range: 48-68 years).

502 Proteins were extracted, separated and transferred onto nitrocellulose membrane (Thermo Fisher
503 Scientific). Rabbit polyclonal anti-VIP antibody (Abcam, Cambridge UK) was used as primary
504 and anti-rabbit HRP-conjugated antibody (Sigma) as secondary. Visualization was performed by
505 ECL Western Blotting Substrate (Thermo Fisher Scientific) on iBrigh FL1500 Imaging System
506 (Invitrogen).

507

508 ***Human VIP protein assessment***

509 Proteins were extracted from 0.5 g of each jejunal sample using TPER tissue protein extraction
510 reagent with protease inhibitor cocktail (Thermo Fisher Scientific). Total protein was quantified
511 using a Nano Drop 2000 spectrophotometer (Thermo Fisher Scientific). Proteins were separated
512 using 12% acrylamide SDS-PAGE in reducing conditions and transferred onto nitrocellulose
513 membrane (Thermo Fisher Scientific) overnight at 12 mV. Membranes were blocked with a buffer
514 containing 5% fat-free milk and then incubated overnight at 4°C with rabbit polyclonal anti-VIP
515 antibody (ab227850; Abcam, Cambridge UK). Anti-rabbit HRP-conjugated secondary antibody
516 (Sigma) was applied 2 hours at room temperature. Immunoreactive bands were visualized by ECL
517 Western Blotting Substrate (Thermo Fisher Scientific) on iBrigh FL1500 Imaging System
518 (Invitrogen). The iBright software was used also to quantify the total protein signal in each lane,

519 stained with Ponceau S, used as reference.

520 ***Statistical analysis***

521 Data analyses were performed using Graphpad Prism 6.0, nSolver 4.0 and Microsoft Excel 2016.
522 Data are presented as medians (IQR) or means±SD, statistical testing was performed using
523 parametric or non-parametric tests, as appropriate.

524

525 **Figure legends**

526 **Figure 1. Gastrointestinal motility in germ-free and colonized mice.**

527 A. Representative photographs of mouse stomach (left) immediately after barium gavage and 3
528 minutes later. Gastric emptying results (right) in conventional (SPF, n=10), germ-free (GF, n=11),
529 *E. coli*-monocolonized (EC, n=8) and *L. rhamnosus*-monocolonized (LR, n=8) mice.

530 B. Representative photographs (left) show only 1 bead in the ileum of a SPF mouse, and 5 beads
531 in the jejunum of a GF mouse. Intestinal transit scores (right) in GF (n=11), SPF (n=10), EC (n=8)
532 and LR (n=8) mice.

533 C,D. KCl- and CCh-induced contractility of tissues from SPF (n=10), GF (n=11), EC (n=8) and
534 LR (n=8) mice. In D, force is expressed as a ratio to KCl-induced contraction in the same tissue.

535 E, F. Representative recordings of EFS-induced responses in tissues from a SPF mouse, with and
536 without the presence of atropine.

537 G,H. EFS-induced relaxation and contraction of tissues from SPF (n=10), GF (n=11), , EC (n=8)
538 and LR (n=8) mice.

539 I. EFS-induced acetylcholine released from tissues of SPF (n=13), GF (n=10), EC (n=12) and LR
540 (n=14) mice, expressed as a ratio to KCl-released acetylcholine in the same tissue.

541

**Figure 2. Neuroimmune genes affected by microbial colonization.**

A, B. Heat map of neuroimmune genes the expression of which differ in whole-thickness jejunum and colon tissues between SPF and GF mice (6 samples per group, each sample contains tissues from 2 mice). Red represents up-regulated genes, blue down-regulated genes, *$p<0.05$, **$p<0.01$.

**Figure 3. Effect of bacterial colonization on myenteric VIP and ChAT.**

A, B. *VIP* and *ChAT* gene expression assessed by Nanostring in tissues from SPF and GF mice (each circle represents a pooled sample from 2 mice).

C. Representative recordings and summary of EFS-induced responses of tissues from SPF mice (n=4), before and after treatment with combined VIP receptor 1 and 2 antagonists.

D. *In vivo* intestinal transit scores of vehicle (n=4) and VIP analogue (n=4) treated SPF mice.

E. VIP- and ChAT-immunoreactive nerves immunolabeled with antibodies to HuC/D (green), VIP (red) and ChAT (cyan) at the jejunal myenteric plexus of a SPF mouse.

F. VIP- and ChAT-immunoreactive nerves visualized by double-immunolabeling with antibodies to VIP (green) and ChAT (red) in jejunal myenteric plexus of SPF (n=4) and GF (n=4) mice.

G. Representative photographs (left) and results (right) of VIP immunoreactivity in the jejunal myenteric plexus of SPF (n=4), GF (n=4), EC (n=4) and LR (n=4) mice.

H. Representative photographs (left) and results (right) of VIP immunoreactivity in the colon myenteric plexus of SPF (n=4) and GF (n=4) mice.

**Figure 4. The role of MYD88/TRIF pathways in intestinal motility and jejunal myenteric VIP.**

A. Intestinal transit scores of SPF C57BL/6 (n=10), SPF *Myd88*$^{-/-}$*Trif*$^{/-}$ (n=18), GF C57BL/6 (n=6), and GF *Myd88*$^{-/-}$*Trif*$^{/-}$ (n=10) mice.

B. EFS-induced responses of jejunum tissues from SPF C57BL/6 (n=8), SPF *Myd88*$^{-/-}$*Trif*$^{/-}$ (n=6) mice GF C57BL/6 (n=11) and GF *Myd88*$^{-/-}$*Trif*$^{/-}$ (n=4) mice.

C. VIP immunoreactivity in the jejunum myenteric plexus of SPF C57BL/6 (n=4), SPF *Myd88*$^{-/-}$ *Trif*$^{/-}$ (n=4), GF C57BL/6 (n=4) and GF *Myd88*$^{-/-}$*Trif*$^{/-}$ (n=4) mice.

D. Representative photographs of VIP immunoreactivity.

E. Intestinal transit scores of GF C57BL/6 and GF *Myd88*$^{-/-}$*Trif*$^{/-}$ mice, before and after monocolonization with *E. coli* (EC, n=6 per group).

F. EFS-induced responses of jejunum tissues from GF C57BL/6 (n=11), GF *Myd88*$^{-/-}$*Trif*$^{/-}$ (n=6), EC C57BL/6 (n=8) and EC *Myd88*$^{-/-}$*Trif*$^{/-}$ (n=6) mice.

G. VIP immunoreactivity of GF C57BL/6 (n=4), GF *Myd88*$^{-/-}$*Trif*$^{/-}$ (n=4), EC C57BL/6 (n=4) and EC *Myd88*$^{-/-}$*Trif*$^{/-}$ (n=6) mice.

H. Representative photographs of VIP immunoreactivity.

**Figure 5. Effect of immune blockade on jejunal myenteric plexus VIP and glial cells.**

A. VIP-immunoreactive nerves and glial cells visualized by double-immunolabeling with antibodies to VIP (green) and glial cells (red, S100β or GFAP) in jejunal myenteric plexus of a SPF mouse.

B. Representative photographs and results of VIP immunoreactivity of *E. coli*-monocolonized mice treated with saline (n=6), fingolimod (n=6) or cosalane (n=6).

C. Representative photographs and results of S100β immunoreactivity (green) of *E. coli*-monocolonized mice treated with saline (n=6), fingolimod (n=6) and cosalane (n=6).

D. Representative photographs and results of S100β immunoreactivity of SPF (n=6) and GF (n=6) and *E. coli*-monocolonized mice (n=6).

E. *In vivo* transit scores of vehicle (n=4) and gliotoxin (n=10) treated SPF mice.

F. Representative photographs and results of VIP immunoreactivity of vehicles (n=5) and gliotoxin applications (n=5) to SPF mice.

**Figure 6. Gut microbiota is essential for normal intestinal transit and jejunal myenteric VIP levels.**

A. Experimental design for permanent colonization of GF mice with *E. coli* JM83 (left); intestinal transit scores for GF mice before (d0), and after colonization with *E.coli* JM83 at day 14 (d14) and day 42 (d42, n=6); VIP expression of GF mice before (d0, n=4), and after colonization with *E.coli* JM83 at day 14 (d14, n=5) and at day 42 (d42, n=6).

B. Experimental design for transient colonization of GF mice with *E. coli* HA107 (left); intestinal transit scores of GF mice (n=11) before and after 2 week-monocolonization (d14) with the transient colonizer *E. coli* HA107, and 4 weeks later, when mice reverted to GF status (d42, n=7); VIP expression of GF mice (n=4), mice monocolonized with *E. coli* HA107 (d14, n=5) and after reverting to GF status (d42, n=8).

C. Experimental design for antibiotic treatment of SPF mice (left); intestinal transit scores of SPF mice before (baseline) and after 1 week of antibiotics (ATB), and after 2 weeks wash-out (2 wks post-ATB, n=8); VIP expression in SPF mice before (n=7) and after antibiotics (n=7) and after 2 weeks wash-out (n=8).

D. Microbiota profiles in antibiotic treated mice. Shannon diversity index and weighted unifrac PCoA plot at baseline, after 1 week of ATB and after 2 weeks wash-out.

E. Total bacterial load at baseline, after 1 week of ATB, and after 2 weeks wash-out period.

F. VIP protein expression in full thickness biopsy jejunum tissues from controls (n=7) and CIPO patients (n=6).

G. Schematic overview of the gut microbiota-neuroimmune interactions governing intestinal

transit.

**References:**


[1] Ma C, Congly SE, Novak KL, Belletrutti PJ, Raman M, Woo M, Andrews CN, Nasser Y. Epidemiologic Burden and Treatment of Chronic Symptomatic Functional Bowel Disorders in the United States: A Nationwide Analysis. Gastroenterology 2021;160(1):88-98 e4.

[2] Margolis KG, Cryan JF, Mayer EA. The Microbiota-Gut-Brain Axis: From Motility to Mood. Gastroenterology 2021;160(5):1486-501.

[3] O'Mahony SM, Felice VD, Nally K, Savignac HM, Claesson MJ, Scully P, Woznicki J, Hyland NP, Shanahan F, Quigley EM, Marchesi JR, O'Toole PW, Dinan TG, Cryan JF. Disturbance of the Gut Microbiota in Early-Life Selectively Affects Visceral Pain in Adulthood without Impacting Cognitive or Anxiety-Related Behaviors in Male Rats. Neuroscience 2014;277:885-901.

[4] Geuking MB, Cahenzli J, Lawson MA, Ng DC, Slack E, Hapfelmeier S, McCoy KD, Macpherson AJ. Intestinal bacterial colonization induces mutualistic regulatory T cell responses. Immunity 2011;34(5):794-806.

[5] Johansson MEV, Gustafsson JK, Holmen-Larsson J, Jabbar KS, Xia LJ, Xu H, Ghishan FK, Carvalho FA, Gewirtz AT, Sjovall H, Hansson GC. Bacteria penetrate the normally impenetrable inner colon mucus layer in both murine colitis models and patients with ulcerative colitis. Gut 2014;63(2):281-91.

[6] Husebye E, Hellstrom PM, Sundler F, Chen J, Midtvedt T. Influence of microbial species on small intestinal myoelectric activity and transit in germ-free rats. American journal of physiology Gastrointestinal and liver physiology 2001;280(3):G368-80.

[7] Berseth CL. Gastrointestinal motility in the neonate. Clin Perinatol 1996;23(2):179-90.

[8] Anitha M, Vijay-Kumar M, Sitaraman SV, Gewirtz AT, Srinivasan S. Gut microbial products regulate murine gastrointestinal motility via Toll-like receptor 4 signaling. Gastroenterology 2012;143(4):1006-16 e4.

[9] Yarandi SS, Kulkarni S, Saha M, Sylvia KE, Sears CL, Pasricha PJ. Intestinal Bacteria Maintain Adult Enteric Nervous System and Nitrergic Neurons via Toll-like Receptor 2-induced Neurogenesis in Mice. Gastroenterology 2020.

[10] Caputi V, Marsilio I, Cerantola S, Roozfarakh M, Lante I, Galuppini F, Rugge M, Napoli E, Giulivi C, Orso G, Giron MC. Toll-Like Receptor 4 Modulates Small Intestine Neuromuscular Function through Nitrergic and Purinergic Pathways. Front Pharmacol 2017;8:350.

[11] De Vadder F, Grasset E, Manneras Holm L, Karsenty G, Macpherson AJ, Olofsson LE,

Backhed F. Gut microbiota regulates maturation of the adult enteric nervous system via enteric serotonin networks. Proc Natl Acad Sci U S A 2018;115(25):6458-63.

[12] Obata Y, Castano A, Boeing S, Bon-Frauches AC, Fung C, Fallesen T, de Aguero MG, Yilmaz B, Lopes R, Huseynova A, Horswell S, Maradana MR, Boesmans W, Vanden Berghe P, Murray AJ, Stockinger B, Macpherson AJ, Pachnis V. Neuronal programming by microbiota regulates intestinal physiology. Nature 2020;578(7794):284-9.

[13] Agace WW, McCoy KD. Regionalized Development and Maintenance of the Intestinal Adaptive Immune Landscape. Immunity 2017;46(4):532-48.

[14] Muller PA, Matheis F, Schneeberger M, Kerner Z, Jove V, Mucida D. Microbiota-modulated CART(+) enteric neurons autonomously regulate blood glucose. Science 2020;370(6514):314-21.

[15] Bercik P, De Giorgio R, Blennerhassett P, Verdu EF, Barbara G, Collins SM. Immune-mediated neural dysfunction in a murine model of chronic Helicobacter pylori infection. Gastroenterology 2002;123(4):1205-15.

[16] De Palma G, Blennerhassett P, Lu J, Deng Y, Park AJ, Green W, Denou E, Silva MA, Santacruz A, Sanz Y, Surette MG, Verdu EF, Collins SM, Bercik P. Microbiota and host determinants of behavioural phenotype in maternally separated mice. Nature communications 2015;6:7735.

[17] Willard AL. A vasoactive intestinal peptide-like cotransmitter at cholinergic synapses between rat myenteric neurons in cell culture. The Journal of neuroscience : the official journal of the Society for Neuroscience 1990;10(3):1025-34.

[18] Matheis F, Muller PA, Graves CL, Gabanyi I, Kerner ZJ, Costa-Borges D, Ahrends T, Rosenstiel P, Mucida D. Adrenergic Signaling in Muscularis Macrophages Limits Infection-Induced Neuronal Loss. Cell 2020;180(1):64-78 e16.

[19] Barajon I, Serrao G, Arnaboldi F, Opizzi E, Ripamonti G, Balsari A, Rumio C. Toll-like receptors 3, 4, and 7 are expressed in the enteric nervous system and dorsal root ganglia. J Histochem Cytochem 2009;57(11):1013-23.

[20] Karmarkar D, Rock KL. Microbiota signalling through MyD88 is necessary for a systemic neutrophilic inflammatory response. Immunology 2013;140(4):483-92.

[21] Fitzgerald KA, Palsson-McDermott EM, Bowie AG, Jefferies CA, Mansell AS, Brady G, Brint E, Dunne A, Gray P, Harte MT, McMurray D, Smith DE, Sims JE, Bird TA, O'Neill LA. Mal (MyD88-adapter-like) is required for Toll-like receptor-4 signal transduction. Nature 2001;413(6851):78-83.

[22] Choi JW, Gardell SE, Herr DR, Rivera R, Lee CW, Noguchi K, Teo ST, Yung YC, Lu M, Kennedy G, Chun J. FTY720 (fingolimod) efficacy in an animal model of multiple

sclerosis requires astrocyte sphingosine 1-phosphate receptor 1 (S1P1) modulation. Proceedings of the National Academy of Sciences of the United States of America 2011;108(2):751-6.

[23] Luessi F, Kraus S, Trinschek B, Lerch S, Ploen R, Paterka M, Roberg T, Poisa-Beiro L, Klotz L, Wiendl H, Bopp T, Jonuleit H, Jolivel V, Zipp F, Witsch E. FTY720 (fingolimod) treatment tips the balance towards less immunogenic antigen-presenting cells in patients with multiple sclerosis. Mult Scler 2015;21(14):1811-22.

[24] Hull-Ryde EA, Porter MA, Fowler KA, Kireev D, Li K, Simpson CD, Sassano MF, Suto MJ, Pearce KH, Janzen W, Coghill JM. Identification of Cosalane as an Inhibitor of Human and Murine CC-Chemokine Receptor 7 Signaling via a High-Throughput Screen. SLAS Discov 2018;23(10):1083-91.

[25] Hapfelmeier S, Lawson MA, Slack E, Kirundi JK, Stoel M, Heikenwalder M, Cahenzli J, Velykoredko Y, Balmer ML, Endt K, Geuking MB, Curtiss R, 3rd, McCoy KD, Macpherson AJ. Reversible microbial colonization of germ-free mice reveals the dynamics of IgA immune responses. Science 2010;328(5986):1705-9.

[26] Bercik P, Denou E, Collins J, Jackson W, Lu J, Jury J, Deng Y, Blennerhassett P, Macri J, McCoy KD, Verdu EF, Collins SM. The intestinal microbiota affect central levels of brain-derived neurotropic factor and behavior in mice. Gastroenterology 2011;141(2):599-609, e1-3.

[27] Crist JR, He XD, Goyal RK. Both ATP and the peptide VIP are inhibitory neurotransmitters in guinea-pig ileum circular muscle. The Journal of physiology 1992;447:119-31.

[28] Fung C, Unterweger P, Parry LJ, Bornstein JC, Foong JP. VPAC1 receptors regulate intestinal secretion and muscle contractility by activating cholinergic neurons in guinea pig jejunum. American journal of physiology Gastrointestinal and liver physiology 2014;306(9):G748-58.

[29] Lelievre V, Favrais G, Abad C, Adle-Biassette H, Lu Y, Germano PM, Cheung-Lau G, Pisegna JR, Gressens P, Lawson G, Waschek JA. Gastrointestinal dysfunction in mice with a targeted mutation in the gene encoding vasoactive intestinal polypeptide: a model for the study of intestinal ileus and Hirschsprung's disease. Peptides 2007;28(9):1688-99.

[30] Shi XZ, Sarna SK. Gene therapy of Cav1.2 channel with VIP and VIP receptor agonists and antagonists: a novel approach to designing promotility and antimotility agents. American journal of physiology Gastrointestinal and liver physiology 2008;295(1):G187-G96.

[31] Krueger D, Michel K, Zeller F, Demir IE, Ceyhan GO, Slotta-Huspenina J, Schemann M.

Neural influences on human intestinal epithelium in vitro. The Journal of physiology 2016;594(2):357-72.

[32] Jayawardena D, Guzman G, Gill RK, Alrefai WA, Onyuksel H, Dudeja PK. Expression and localization of VPAC1, the major receptor of vasoactive intestinal peptide along the length of the intestine. American journal of physiology Gastrointestinal and liver physiology 2017;313(1):G16-G25.

[33] Wu X, Conlin VS, Morampudi V, Ryz NR, Nasser Y, Bhinder G, Bergstrom KS, Yu HB, Waterhouse CC, Buchan AM, Popescu OE, Gibson WT, Waschek JA, Vallance BA, Jacobson K. Vasoactive intestinal polypeptide promotes intestinal barrier homeostasis and protection against colitis in mice. PLoS One 2015;10(5):e0125225.

[34] Ignacio A, Morales CI, Camara NO, Almeida RR. Innate Sensing of the Gut Microbiota: Modulation of Inflammatory and Autoimmune Diseases. Frontiers in immunology 2016;7:54.

[35] Yamamoto M, Sato S, Hemmi H, Hoshino K, Kaisho T, Sanjo H, Takeuchi O, Sugiyama M, Okabe M, Takeda K, Akira S. Role of adaptor TRIF in the MyD88-independent toll-like receptor signaling pathway. Science 2003;301(5633):640-3.

[36] Fowler KA, Li K, Whitehurst CB, Bruce DW, Moorman NJ, Aube J, Coghill JM. The Ex Vivo Treatment of Donor T Cells with Cosalane, an HIV Therapeutic and Small-Molecule Antagonist of CC-Chemokine Receptor 7, Separates Acute Graft-versus-Host Disease from Graft-versus-Leukemia Responses in Murine Hematopoietic Stem Cell Transplantation Models. Biol Blood Marrow Transplant 2019;25(6):1062-74.

[37] Lee CW, Choi JW, Chun J. Neurological S1P signaling as an emerging mechanism of action of oral FTY720 (fingolimod) in multiple sclerosis. Arch Pharm Res 2010;33(10):1567-74.

[38] Chun J, Hartung HP. Mechanism of action of oral fingolimod (FTY720) in multiple sclerosis. Clin Neuropharmacol 2010;33(2):91-101.

[39] Zeng X, Wang T, Zhu C, Xing X, Ye Y, Lai X, Song B, Zeng Y. Topographical and biological evidence revealed FTY720-mediated anergy-polarization of mouse bone marrow-derived dendritic cells in vitro. PLoS One 2012;7(5):e34830.

[40] Gulbransen BD, Sharkey KA. Novel functional roles for enteric glia in the gastrointestinal tract. Nature reviews Gastroenterology & hepatology 2012;9(11):625-32.

[41] Sharkey KA. Emerging roles for enteric glia in gastrointestinal disorders. The Journal of clinical investigation 2015;125(3):918-25.

[42] Mowat AM, Agace WW. Regional specialization within the intestinal immune system. Nature Reviews Immunology 2014;14(10):667-85.

[43] Seguella L, Gulbransen BD. Enteric glial biology, intercellular signalling and roles in gastrointestinal disease. Nat Rev Gastro Hepat 2021;18(8):571-87.

[44] Hung LY, Boonma P, Unterweger P, Parathan P, Haag A, Luna RA, Bornstein JC, Savidge TC, Foong JPP. Neonatal Antibiotics Disrupt Motility and Enteric Neural Circuits in Mouse Colon. Cellular and molecular gastroenterology and hepatology 2019;8(2):298-300 e6.

[45] Di Nardo G, Di Lorenzo C, Lauro A, Stanghellini V, Thapar N, Karunaratne TB, Volta U, De Giorgio R. Chronic intestinal pseudo-obstruction in children and adults: diagnosis and therapeutic options. Neurogastroenterology and motility : the official journal of the European Gastrointestinal Motility Society 2017;29(1).

[46] Koch TR, Carney JA, Go L, Go VL. Idiopathic chronic constipation is associated with decreased colonic vasoactive intestinal peptide. Gastroenterology 1988;94(2):300-10.

[47] Sohn W, Lee OY, Lee SP, Lee KN, Jun DW, Lee HL, Yoon BC, Choi HS, Sim J, Jang KS. Mast cell number, substance P and vasoactive intestinal peptide in irritable bowel syndrome with diarrhea. Scand J Gastroenterol 2014;49(1):43-51.

[48] Gu L, Ding C, Tian H, Yang B, Zhang X, Hua Y, Zhu Y, Gong J, Zhu W, Li J, Li N. Serial Frozen Fecal Microbiota Transplantation in the Treatment of Chronic Intestinal Pseudo-obstruction: A Preliminary Study. J Neurogastroenterol Motil 2017;23(2):289-97.

[49] El-Salhy M, Hatlebakk JG, Gilja OH, Brathen Kristoffersen A, Hausken T. Efficacy of faecal microbiota transplantation for patients with irritable bowel syndrome in a randomised, double-blind, placebo-controlled study. Gut 2020;69(5):859-67.

[50] De PG, Blennerhassett P, Lu J, Deng Y, Park AJ, Green W, Denou E, Silva MA, Santacruz A, Sanz Y, Surette MG, Verdu EF, Collins SM, Bercik P. Microbiota and host determinants of behavioural phenotype in maternally separated mice. Nat Commun 2015;6:7735.

[51] Bercik P, Wang L, Verdu EF, Mao YK, Blennerhassett P, Khan WI, Kean I, Tougas G, Collins SM. Visceral hyperalgesia and intestinal dysmotility in a mouse model of postinfective gut dysfunction. Gastroenterology 2004;127(1):179-87.

[52] Jacobson K, McHugh K, Collins SM. The mechanism of altered neural function in a rat model of acute colitis. Gastroenterology 1997;112(1):156-62.

[53] Vallance BA, Blennerhassett PA, Collins SM. Increased intestinal muscle contractility and worm expulsion in nematode-infected mice. The American journal of physiology 1997;272(2 Pt 1):G321-7.

[54] Igarashi H, Ito T, Mantey SA, Pradhan TK, Hou W, Coy DH, Jensen RT. Development of simplified vasoactive intestinal peptide analogs with receptor selectivity and stability for human vasoactive intestinal peptide/pituitary adenylate cyclase-activating polypeptide

receptors. Journal of Pharmacology and Experimental Therapeutics 2005;315(1):370-81.

[55] Hayakawa K, Nakano T, Irie K, Higuchi S, Fujioka M, Orito K, Iwasaki K, Jin G, Lo EH, Mishima K, Fujiwara M. Inhibition of reactive astrocytes with fluorocitrate retards neurovascular remodeling and recovery after focal cerebral ischemia in mice. J Cereb Blood Flow Metab 2010;30(4):871-82.

[56] Bartram AK, Lynch MD, Stearns JC, Moreno-Hagelsieb G, Neufeld JD. Generation of multimillion-sequence 16S rRNA gene libraries from complex microbial communities by assembling paired-end illumina reads. Appl Environ Microbiol 2011;77(11):3846-52.

[57] Whelan FJ, Surette MG. A comprehensive evaluation of the sl1p pipeline for 16S rRNA gene sequencing analysis. Microbiome 2017;5(1):100.

[58] Callahan BJ, McMurdie PJ, Rosen MJ, Han AW, Johnson AJ, Holmes SP. DADA2: High-resolution sample inference from Illumina amplicon data. Nat Methods 2016;13(7):581-3.

[59] Bolyen E, Rideout JR, Dillon MR, Bokulich NA, Abnet CC, Al-Ghalith GA, Alexander H, Alm EJ, Arumugam M, Asnicar F, Bai Y, Bisanz JE, Bittinger K, Brejnrod A, Brislawn CJ, Brown CT, Callahan BJ, Caraballo-Rodriguez AM, Chase J, Cope EK, Da Silva R, Diener C, Dorrestein PC, Douglas GM, Durall DM, Duvallet C, Edwardson CF, Ernst M, Estaki M, Fouquier J, Gauglitz JM, Gibbons SM, Gibson DL, Gonzalez A, Gorlick K, Guo J, Hillmann B, Holmes S, Holste H, Huttenhower C, Huttley GA, Janssen S, Jarmusch AK, Jiang L, Kaehler BD, Kang KB, Keefe CR, Keim P, Kelley ST, Knights D, Koester I, Kosciolek T, Kreps J, Langille MGI, Lee J, Ley R, Liu YX, Loftfield E, Lozupone C, Maher M, Marotz C, Martin BD, McDonald D, McIver LJ, Melnik AV, Metcalf JL, Morgan SC, Morton JT, Naimey AT, Navas-Molina JA, Nothias LF, Orchanian SB, Pearson T, Peoples SL, Petras D, Preuss ML, Pruesse E, Rasmussen LB, Rivers A, Robeson MS, 2nd, Rosenthal P, Segata N, Shaffer M, Shiffer A, Sinha R, Song SJ, Spear JR, Swafford AD, Thompson LR, Torres PJ, Trinh P, Tripathi A, Turnbaugh PJ, Ul-Hasan S, van der Hooft JJJ, Vargas F, Vazquez-Baeza Y, Vogtmann E, von Hippel M, Walters W, Wan Y, Wang M, Warren J, Weber KC, Williamson CHD, Willis AD, Xu ZZ, Zaneveld JR, Zhang Y, Zhu Q, Knight R, Caporaso JG. Reproducible, interactive, scalable and extensible microbiome data science using QIIME 2. Nat Biotechnol 2019;37(8):852-7.

[60] McMurdie PJ, Holmes S. phyloseq: an R package for reproducible interactive analysis and graphics of microbiome census data. PLoS One 2013;8(4):e61217.

[61] Wang Q, Garrity GM, Tiedje JM, Cole JR. Naive Bayesian classifier for rapid assignment of rRNA sequences into the new bacterial taxonomy. Appl Environ Microbiol 2007;73(16):5261-7.

[62] DeSantis TZ, Hugenholtz P, Larsen N, Rojas M, Brodie EL, Keller K, Huber T, Dalevi D,

825 Hu P, Andersen GL. Greengenes, a chimera-checked 16S rRNA gene database and
826 workbench compatible with ARB. Appl Environ Microbiol 2006;72(7):5069-72.

827

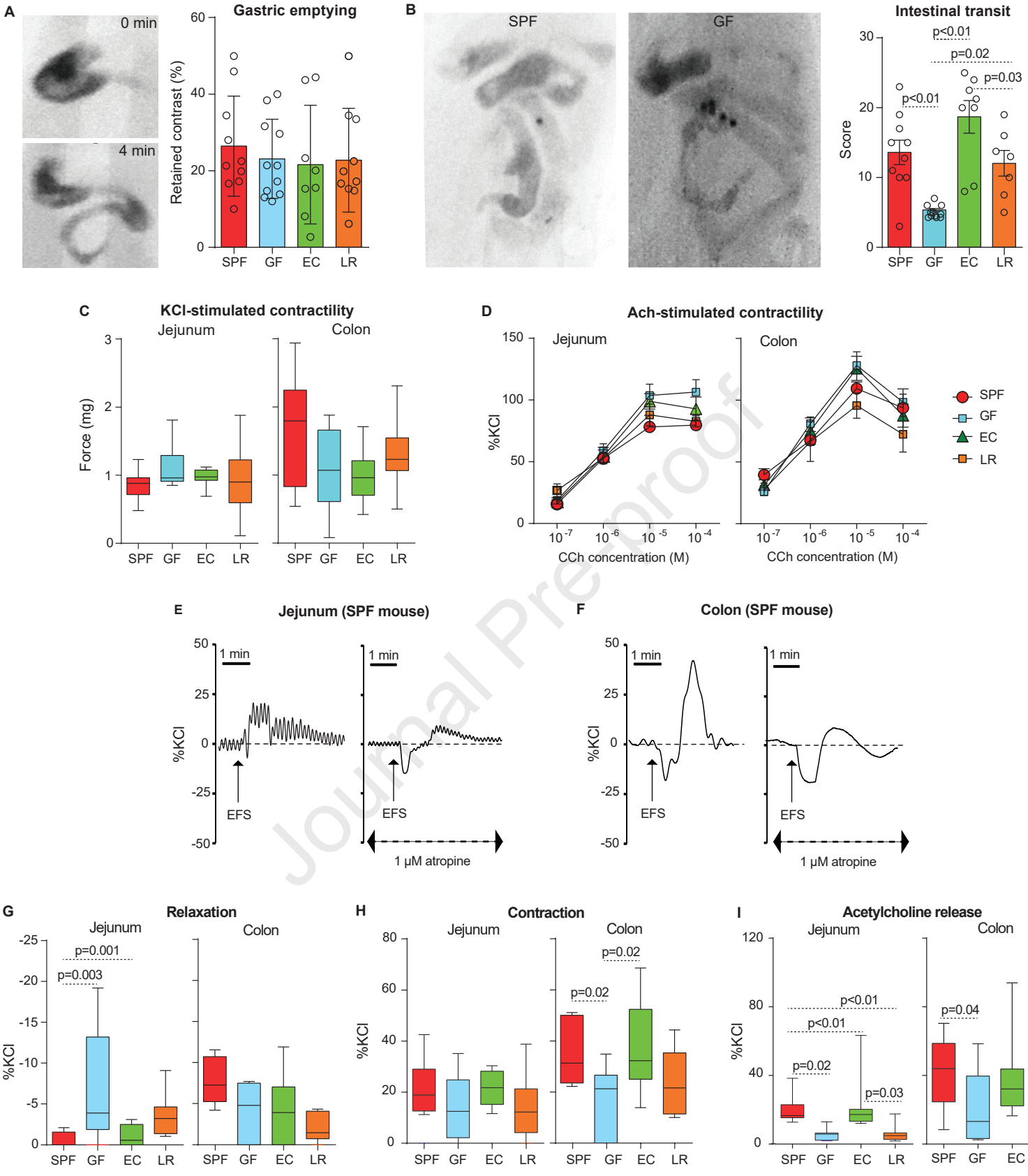

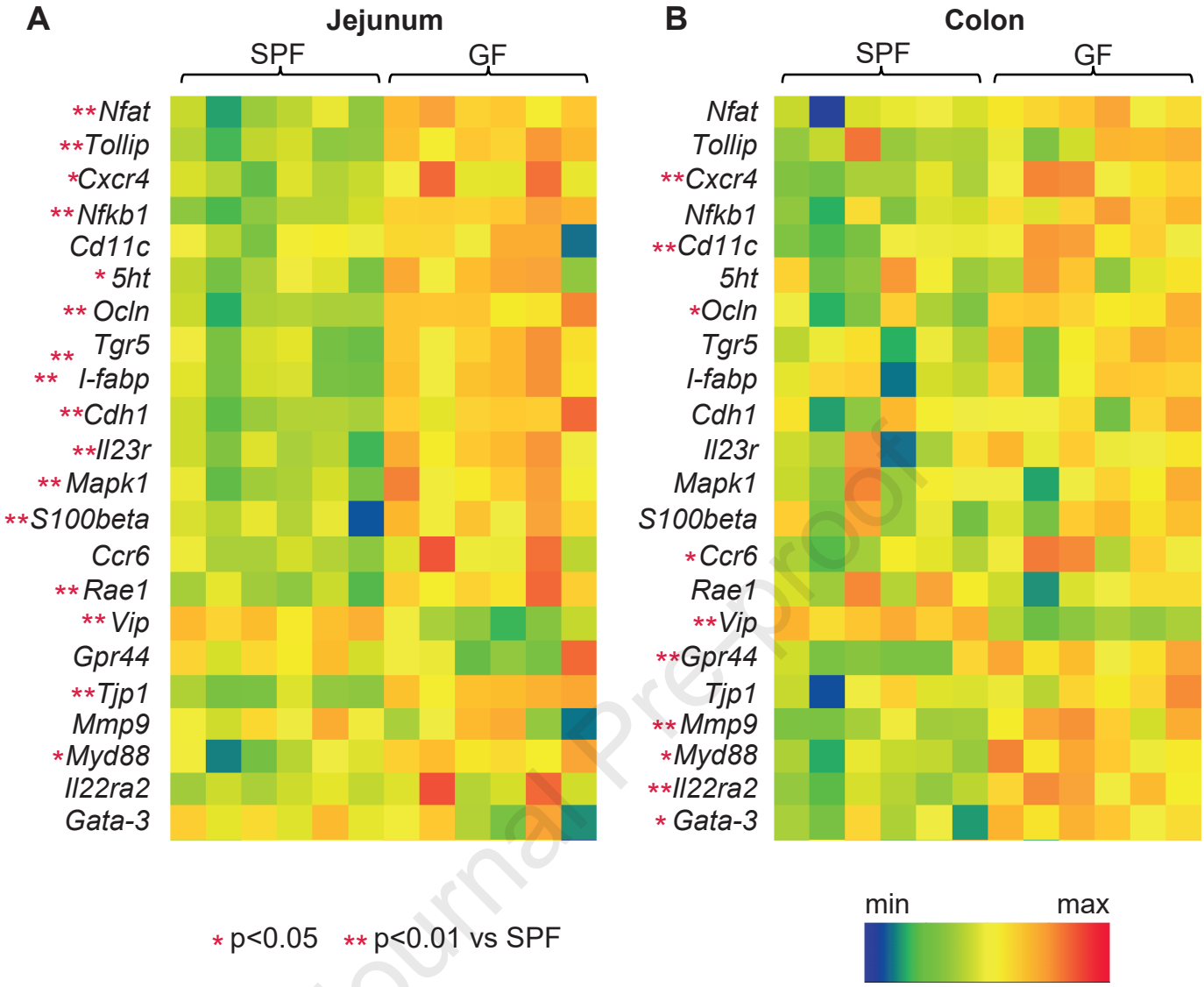

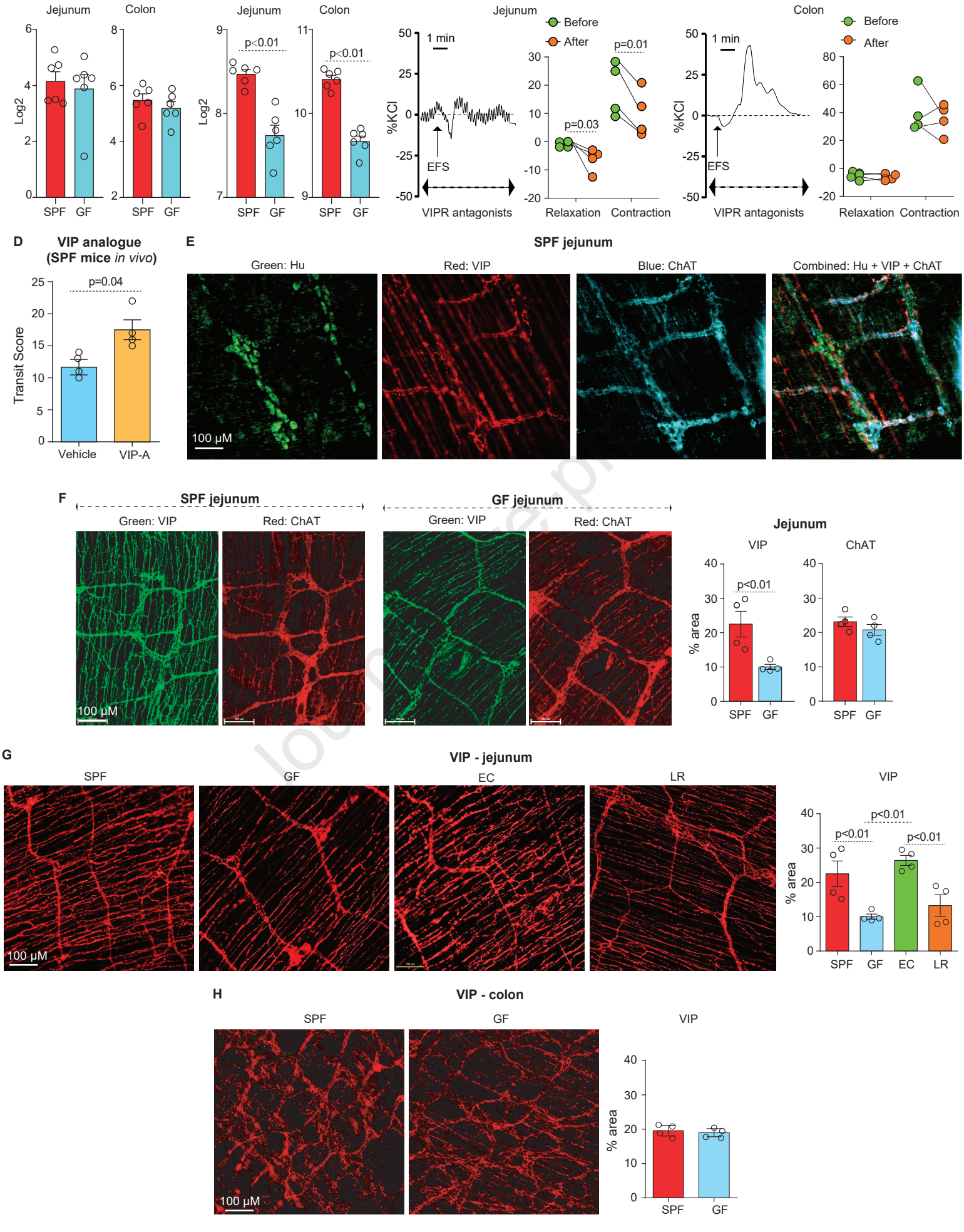

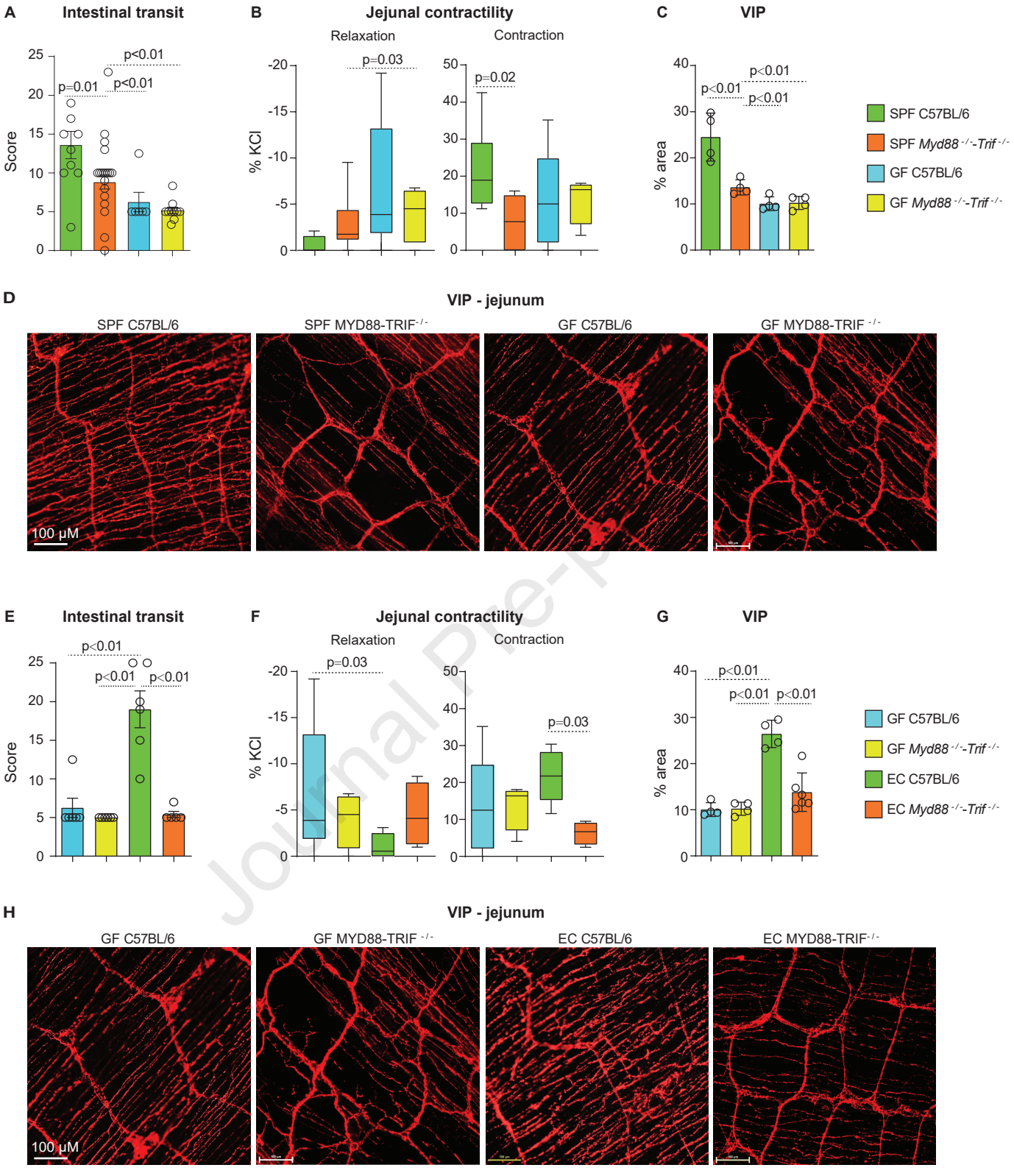
A
Intestinal transit
Score
p=0.01
p<0.01
p<0.01
B
Jejunal contractility
Relaxation
Contraction
% KCl
p=0.03
p=0.02
C
VIP
% area
p<0.01
p<0.01
p<0.01
SPF C57BL/6
SPF Myd88 -/--Trif -/-
GF C57BL/6
GF Myd88 -/--Trif -/-
D
VIP - jejunum
SPF C57BL/6
SPF MYD88-TRIF -/-
GF C57BL/6
GF MYD88-TRIF -/-
100 µM
E
Intestinal transit
Score
p<0.01
p<0.01
p<0.01
F
Jejunal contractility
Relaxation
Contraction
% KCl
p=0.03
p=0.03
G
VIP
% area
p<0.01
p<0.01
p<0.01
GF C57BL/6
GF Myd88 -/--Trif -/-
EC C57BL/6
EC Myd88 -/--Trif -/-
H
VIP - jejunum
GF C57BL/6
GF MYD88-TRIF -/-
EC C57BL/6
EC MYD88-TRIF -/-
100 µM